DOI: 10.1111/cgf.70126
Eurographics Conference on Visualization (EuroVis) 2025
W. Aigner, N. Andrienko, and B. Wang
(Guest Editors)

COMPUTER GRAPHICS *forum*
Volume 44 (2025), Number 3

Euclidean, Hyperbolic, and Spherical Networks: An Empirical Study of Matching Network Structure to Best Visualizations

Jacob Miller[1], Dhruv Bhatia[2], Helen Purchase[3], and Stephen Kobourov[1,2]

[1]Technical University of Munich, Germany
[2]University of Arizona, USA
[3]Monash University, Australia

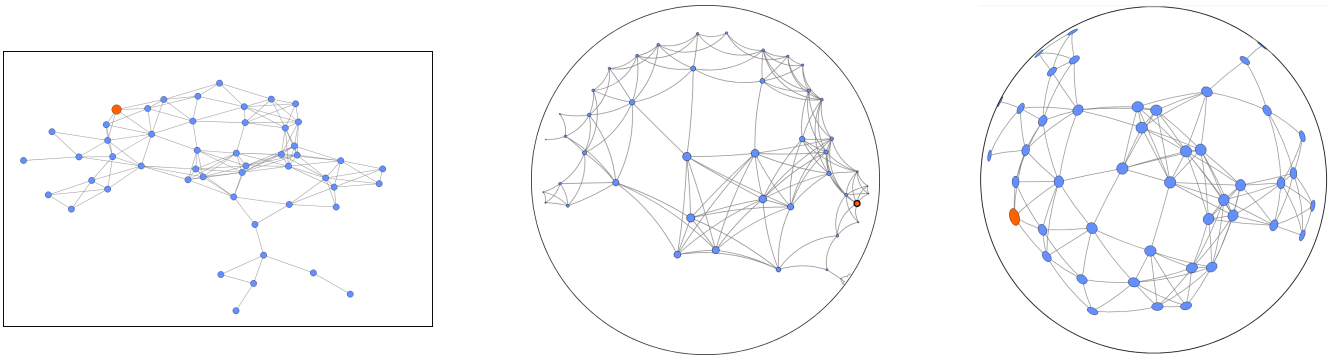

(a) (b) (c)

Figure 1: *The same network visualized in three geometries present in our study: (a) Euclidean, (b) hyperbolic, (c) spherical.*

Abstract

We investigate the usability of Euclidean, spherical and hyperbolic geometries for network visualization. Several techniques have been proposed for both spherical and hyperbolic network visualization tools, based on the fact that some networks admit lower embedding error (distortion) in such non-Euclidean geometries. However, it is not yet known whether a lower embedding error translates to human subject benefits, e.g., better task accuracy or lower task completion time. We design, implement, conduct, and analyze a human subjects study to compare Euclidean, spherical and hyperbolic network visualizations using tasks that span the network task taxonomy. While in some cases accuracy and response times are negatively impacted when using non-Euclidean visualizations, the evaluation shows that differences in accuracy for hyperbolic and spherical visualizations are not statistically significant when compared to Euclidean visualizations. Additionally, differences in response times for spherical visualizations are not statistically significant compared to Euclidean visualizations.

CCS Concepts

• ***Human-centered computing*** → ***Visualization design and evaluation methods;*** *Empirical studies in visualization;*

1. Introduction

Many network visualizations begin with a node-link diagram drawn in the Euclidean plane, such as the space of the computer screen or a sheet of paper. However, representations in different geometries have shown visualization benefits, for example focus+context effects and the possibility to represent the underlying data more faithfully. In the context of network visualization, spherical [GSF97,KW05,SK03], hyperbolic [MB95,Mun97,LRP95], and toroidal [CDMB20,CDBM21] geometries have been considered.

Although these visualizations differ significantly from the standard Euclidean setting, there has been little work in evaluating their performance with human subjects studies. Thus, there is little one can say about when it is appropriate to make use of such non-Euclidean network visualizations. Early results comparing spherical, hyperbolic and Euclidean network visualizations indicate some benefits [DCL*17]; in this paper we expand the types of tasks and use consistent embedding methods. Spherical and toroidal geometries have been shown to aid in cluster identification tasks [CDY*22]. In contrast, we consider Euclidean, hyperbolic, and spherical visualizations and different types of networks.

Unlike the well-known embedding-quality metric stress [Kru64, EMK*21], distortion [SSGR18, MKH22] can be used to compare the quality of embeddings between different geometries. Previous work has shown that some networks can be embedded with lower distortion in non-Euclidean spaces [SSGR18] and there exist algorithms which consistently achieve this lower distortion for both

spherical [MHK23] and hyperbolic [MKH22] spaces. We aim to verify if this helps with task performance (time or accuracy).

Recent human subjects studies have confirmed that people can perceive differences in stress/distortion [MPW*24], which leads to the question whether the lower distortion realizable by some network/geometry pairs corresponds to visualization benefits, such as task support or aesthetic preference. In this paper we describe a human subjects study to answer the following research questions:

- **RQ1**: Does the distortion of a network embedding correspond to better task support, i.e., if the embedding has the lowest distortion in hyperbolic space, is there measurable benefit to using hyperbolic space?
- **RQ2**: What is the effect of using non-Euclidean network visualizations over the traditional Euclidean setting, i.e., how are task accuracy and response time affected?
- **RQ3**: Are some tasks better suited to a particular visualization geometry?

Our study covers many types of network tasks and includes networks defined from Euclidean, spherical, and hyperbolic spaces, unlike prior studies that focus on a subset of possible tasks and on particular network types. We expect a network taken from a space will be better suited to task support when visualized in that space. We show that while the use of non-Euclidean geometries requires more interactions, there is no adverse effect in time and accuracy overall compared to Euclidean visualizations. This partially confirms and partially conflicts with results from earlier studies [DCL*17, CDY*22]. In particular, our contributions are:

- To the best of our knowledge, the first human subjects study on non-Euclidean network visualization to account for network structure and to use comparable layout algorithms.
- Partially confirming results by Du et al. [DCL*17] that spherical network visualizations are comparable to traditional Euclidean visualizations, but now of a full spectrum on 6 network tasks.
- New results showing that while hyperbolic visualizations tend to have longer response times, they are comparable for networks with hyperbolic structure.
- An exploratory analysis of participant accuracy and response time by task in each geometry.
- Summary of qualitative participant responses which indicate, among other things, that the hyperbolic visualization style was polarizing among participants.

2. Background and Related Work

We give a brief background on non-Euclidean geometry, its use in network visualization, and related work we build upon in this paper.

2.1. Background

Consistent geometries are the spaces which satisfy the first four of Euclid's postulates from his classical *Elements* text: Euclidean, hyperbolic, and spherical (elliptical) geometries. Non-Euclidean geometries refer to both hyperbolic and spherical geometries, which are obtained by modifying Euclid's fifth postulate about parallel lines. Two lines A and B are said to be parallel if there is a third line, C, which intersects them both at right angles. In Euclidean geometry, the distance between A and B remains a fixed constant. The behavior is different in non-Euclidean geometries: in hyperbolic space, A and B will "curve away" and increase in distance the further from the intersection of C while in spherical space, A and B "curve into" each other eventually intersecting.

Non-Euclidean geometries have an interesting history with network visualization dating back to the 1990s. They were first introduced with hyperbolic browsers for tree visualization, by Lamping et al. [LRP95] and Munzner [MB95, Mun97]. Meanwhile, spherical geometry was used for force-directed network layout [GSF97, KW05, PYGK20] and for self-organizing maps [SK03, WT06].

The network visualizations in our system that are seen in multiple figures throughout the paper (e.g. Fig. 1) are based on Multi-Dimensional Scaling (MDS) for network drawing. MDS was first introduced for statistical analysis of data [Tor52], but has since become a popular dimension reduction [EMK*21] technique. MDS was first applied to network drawing by Kamada and Kawai [KK89] and later improved via stress majorization in [GKN04]. More recently, it has been shown that stochastic gradient descent is more consistent and requires fewer iterations to reach minimum stress levels than the stress majorization algorithm [ZPG19].

MDS can be extended to non-Euclidean geometries [MKH22, MHK23]. As in Euclidean space, the goal is to match the graph-theoretic distances in the network to the geodesic distances (shortest distance between two points in the respective geometry) in the drawing space. A metric known as distortion [SSGR18, MKH22] represents how well these graph-theoretic distances are preserved in the embedding. The distortion function (similar to the more familiar notion of stress) allows us to compare the quality of the embedding across different geometries and is defined as follows:

$$\binom{|V|}{2}^{-1} \Sigma_{i<j} \frac{|\delta(X_i, X_j) - d_{i,j}|}{d_{i,j}} \tag{1}$$

where X_i represents the position of vertex i in the drawing space, $d_{i,j}$ is the graph-theoretic distance between vertex i and vertex j, and δ is the geodesic distance function between two points. Sala et al. [SSGR18] show that certain networks (e.g. trees) can be embedded with lower distortion in hyperbolic space than is possible in Euclidean space. Similarly, there are networks that can be embedded with lower distortion on the sphere (e.g., 3-dimensional polytopes). Miller et al. show that lower distortion embeddings can be computed efficiently with the hyperbolic MDS algorithm [MKH22] and with the spherical MDS algorithm [MHK23].

2.2. Related Work

Yoghourdjian et al. [YAD*18] summarize and categorize over 100 papers that involve human subjects empirical studies in network visualization. They consider different features such as complexity, tasks, interactions, and size, with one of the key takeaways being that only 37% of studies in the survey used networks with more than 100 nodes. The size and number of networks used in our study is consistent with the state-of-the-art found by Yoghoudjian et al.

A survey on non-Euclidean network visualization identifies several open areas of research [MBK24], specifically noting the lack

of human subjects studies conducted in this field, despite the positive conclusions of a handful of earlier experiments with spherical [DCL*17] and toroidal [CDBM21, CDY*22] visualizations. Recently, Jeon et al. call on the visualization and HCI communities to further investigate the validity of non-Euclidean visualization through human subjects studies [JLK*25]. We aim to fill in some of the gaps in studies on spherical and hyperbolic visualizations.

We build on a previous study by Du et al. [DCL*17], who introduced iSphere, which maps a Euclidean drawing onto the sphere using inverse projections. A within-subjects user study then compares Euclidean against hyperbolic and spherical layouts. Participants are presented with layouts of stochastic block model random networks (networks with clusters), and are asked to solve network tasks in each of the three visualization styles. The layouts were derived from a stress majorization for Euclidean [GKN04], a force-directed algorithm for hyperbolic [KW05], and the iSphere technique for the sphere [DCL*17]. In Du et al.'s study, participants were presented with three tasks related to node degrees:

- **D1** Given a node A, find a target node B with the highest degree in A's neighborhood.
- **D2** Given two nodes A and B, find a target node C with the highest degree among the common neighbors of A and B.
- **D3** Given a path from node A to node B, find a target node C with the highest degree among the nodes on the path.

The study considers different screen sizes and network sizes as additional dependent variables with the primary variable being the visualization style. Each network had 3 clusters, with low or high network modularity (a network statistic quantifying cluster density). The main results indicate that the sphere and Euclidean visualizations provide comparable time and accuracy, while hyperbolic performed worse in some tasks. In particular, no significant differences were found between any of the three conditions for tasks **D1** and **D2**, while the hyperbolic condition was associated with significantly worse time and accuracy for task **D3**. Additionally, participants in the experiment consistently ranked the hyperbolic condition worse than both the Euclidean and spherical conditions.

Compared to the study of Du et al., ours offers several improvements. First, we use 6 tasks that better cover the spectrum in the network (graph) task taxonomy. Second, we use a consistent set of embedding algorithms across the three geometries: all layouts are MDS-based and optimize the same function in each geometry. Third, we use a more diverse set of networks, including networks specifically chosen because they can be embedded with lower distortion in each of the 3 geometries.

Chen [CHE22] describes a systematic exploration of the design space for wrappable visualizations, which includes spherical and toroidal network visualizations, but not hyperbolic visualizations. Chen et al. [CDBM21] compare several different drawing styles on the torus to the Euclidean plane and find that toroidal drawings have benefits in cluster identification tasks. Another study comparing Euclidean, toroidal, and several spherical visualization styles also finds that toroidal and spherical drawing styles outperform Euclidean drawings for cluster identification tasks [CDY*22].

Lens effects are visually similar to non-Euclidean visualizations. Fisheye views for networks were introduced by Sarkar and Brown [SB94] and have been used to provide focus+context in network visualizations. A user study by Wang et al. [WWZ*19] measures time and accuracy between flat drawings, a hyperbolic visualization, the iSphere technique [DCL*17], and the authors' own fisheye technique. The authors partially replicate some results from Du et al. [DCL*17] and observe that the fisheye view provided the lowest error and completion times with their data.

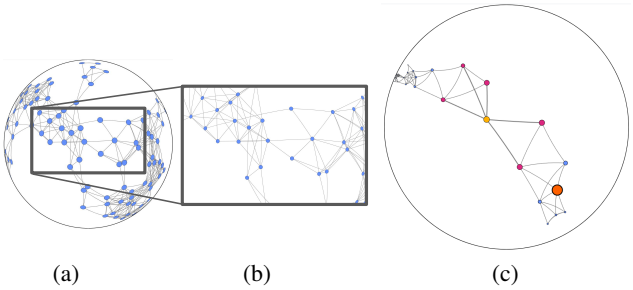

Figure 2: *Illustration of zooming in condition **S**: (a) is the default size (b) shows a zoomed-in view on the center. (c) Hovering over a node changes its color to yellow. All neighbor colors also change to magenta. Edges between the hovered node and its neighbors are emphasized by increased thickness.*

We classify the tasks used in our experiment along two dimensions of taxonomies: Lee et al. [LPP*06] provide a network task taxonomy which covers network-specific tasks at both a high and low level. Specifically, we use four topology-based tasks (adjacency, accessibility, common connection, connectivity) along with an overview task. Low level tasks for general data visualization are also applicable to networks in many cases, so we additionally classify our tasks with the taxonomy by Amar et al. [AES05]. Specifically, our tasks include filtering, retrieving a value, comparing values, finding extrema, and determining range. Table 2 shows how our tasks fit in these two taxonomies.

3. Methodology and Design

In this section we detail our experimental design. We were guided by prior human subjects studies about network visualization, extensive piloting, and the need to keep the study to a reasonable length. Our research questions posed in the introduction were the primary factors in our study design. These questions are informed by recent work [MHK23, MKH22] with the goal to extend the previous Du et al. study [DCL*17]. For **RQ1** it is necessary to include a wide variety of networks in the experiment; for each geometry there should be network embeddings for which their distortion is lowest in that geometry. **RQ2** guides us to a within-subjects study design, so that we can compare a baseline (Euclidean) to the other visualization conditions. Finally, **RQ3** suggests we should include a broad spectrum of network tasks.

3.1. Conditions

The conditions of interest are the geometries of the visualization: Euclidean, spherical, and hyperbolic. As much as feasible, the con-

ditions differ only in the behaviour of the geometry with care taken to ensure everything else remains the same.

Euclidean (E): The Euclidean condition represents a standard node-link diagram, drawn in the flat, 2D space of the computer screen. Nodes are drawn as circles and edges drawn as straight line segments between the adjacent nodes. Node radius is set to 10 pixels, with edge width set to 1.5 pixels. The drawing is scaled so that it just fits the viewing window upon start. The border of the viewing window is drawn as 1 pixel wide black line, indicating the boundary. An example is shown in Fig. 1(a).

Hyperbolic(H): For the hyperbolic condition the network is first embedded in hyperbolic space and then node positions on the computer screen are computed using a Poincarè projection. Nodes are still drawn as circles, with edges becoming circular arc segments, which represent geodesics in hyperbolic space. In the Poincarè projection, lengths and areas decrease at an exponential rate with the distance from the center of the view. For this reason, while nodes in the center of the projection have a radius of 10 pixels, they get smaller the further from the center they are. Similarly, edge width is 1.5 pixels near the center, and decreases away from it. The boundary of the disk is drawn with a solid 1 pixel black circle. An example is shown in Fig. 1(b).

Spherical (S): For the spherical condition the network is first embedded on a sphere and the view provided shows half of the sphere (the "view-from-space" orthographic projection). Nodes are drawn as circles with 10 pixel radius at the center, but due to the projection become ellipses near the boundary. Edges are circular arc segments that represent geodesics in spherical space. The width of the edges is 1.5 pixels. The boundary of the projection is drawn with a solid 1 pixel black circle. Unique to the sphere, due to the orthographic projection, half of the drawing space is always obscured at one time. An example is shown in Fig. 1(c).

3.2. Interactions

Introducing interactions also introduces complexity and potentially confounding factors. However, some interactions are needed in order to make task-solving feasible, especially in the **H** and **S** conditions. We provide a small set of interactions (pan, zoom, hover, recenter, reset) as described below. Note that none of these interactions affect the quality of the embedding (measured by its distortion value), although some visually change the embedding (e.g., the fisheye view effect of recentering in hyperbolic space). We record all interactions by a participant, and utilize them in our analysis.

Pan The geometric pan interaction allows users to bring an area of interest in the center. It is implemented via the standard "grab and drag" fashion in all three conditions. This is done via translation (**E**), Möbius transformation (**H**) [MKH22], and rotation (**S**). Panning is a common interaction employed in prior network visualization studies [DCL*17, PCZ*21, SZG*96].

Zoom Zooming is another common interaction that is particularly useful for networks with more than a few dozen vertices [DCL*17, WWZ*19]. There are two different notions of zoom

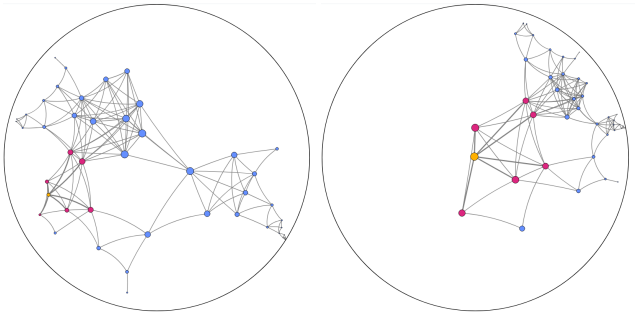

(a) (b)

Figure 3: *Re-centering a node by double-clicking on it: (a) shows a node which is to be re-centered (yellow) and (b) shows the yellow node brought to the center of viewing window. This action is smoothly interpolated from the start to end positions.*

in non-Euclidean geometries [MKH22]. In Euclidean space, zooming is akin to bringing the plane closer to the viewer, so our implementation is analogous for non-Euclidean spaces (bringing the sphere or hyperbolic plane closer); see Fig. 2.

Recenter around click A interaction typically present in hyperbolic browsing systems [MKH22] is the recenter interaction. When the user double-clicks on a point, the system automatically pans to make the clicked point the center of the layout. This interaction is provided in all three conditions. An example is shown in Fig. 3.

Hover Early feedback indicated that participants were unsure exactly where they were clicking to perform the recenter interaction. With this in mind, we provided a hover interaction. When the mouse cursor enters the boundary of a node, the node color changes, the boundary and incident edges are thickened and the neighbors change color. The benefits of static and motion highlighting of nodes and their neighbors in node-link diagrams, especially when solving visual tasks such as ours, have been studied before [MCH*09, WB05]; see Fig. 2.

Reset visualization Early participant feedback indicated that too much zooming/panning, can get one "lost in space", especially in the hyperbolic condition where the entire network can become invisible if forced too far from the center. This justified the reset button which restores the initial state of the visualization.

3.3. Fixed parameters

Here we discuss the fixed parameters of the experiment including the data (networks, layout) and aesthetic choices (sizes, colors).

Networks The selection of networks was a careful choice in order to be able to effectively answer **RQ1**. We initially intended to use only real-world networks taken from Miller et al. [MHK23] but ultimately decided that controlling for size and density was desirable for most networks to reduce confounding factors. For each geometry, we generated two random networks based on the Random Geometric Graph generator for Euclidean space [Pen03], which has already been generalized to hyperbolic space [KPK*10] and generalizes naturally to the sphere. These models uniformly distribute

	|V|	|E|	avg_deg.	**E**_dist.	**H**_dist.	**S**_dist.
E_rand_s	50	150	6.0000	**0.1033**	0.1362	0.1217
E_rand_l	100	400	8.0000	**0.1011**	0.1312	0.1495
dwt_162	162	510	6.2963	**0.0928**	0.2217	0.1191
H_rand_s	50	150	6.0000	0.2465	**0.0913**	0.1143
H_rand_l	100	400	8.0000	0.2459	**0.1234**	0.1829
tree_150	150	149	1.9867	0.2815	**0.1514**	0.2068
S_rand_s	50	150	6.0000	0.2443	0.1121	**0.0897**
S_rand_l	100	400	8.0000	0.2450	0.1439	**0.1060**
dodec_3	230	240	2.0870	0.3014	0.3615	**0.0544**

Table 1: *Summary of the networks that appeared in our experiment along with their embedding scores in each geometry. Accompanying images of each network and layout can found in supplementary material.*

$|V|$ points in the desired geometry, then connect two points with an edge if they are within a geodesic radius r.

We slightly modify this procedure by only taking the *first* $|E|$ shortest edges (sorted by length). In this way, we can specify both $|V|$ and $|E|$ to obtain the desired size and density while still capturing the target space. We also ensure that all generated networks are connected. These networks are named E_rand_small, E_rand_large, and similar for **S** and **H**; see Table 1. We confirmed that the distortion values of the embeddings were indeed lower in the appropriate geometry, compared to the other geometries. While these networks are random, they fundamentally differ in the geometry they are derived from. It has been shown that geometric random networks from a non-Euclidean space exhibit properties not found in other random networks [KPK*10], and such networks allow us to answer **RQ1** – do networks with lower distortion in a particular geometry benefit when visualized in that geometry?

We included three networks representative of the types of networks that can be embedded with low distortion in their "natural geometry". Euclidean space is natural for the wire mesh network *dwt_162*. Hyperbolic space is natural for a tree on 150 nodes, *tree_150*. Spherical space is natural for the network representation of the planar solid dodecahedron, subdivided three times, *dodecahedron_3*. These networks are also summarized in Table 1 and seen in Fig. 4.

Network Layout The layout algorithms used were chosen carefully to be as similar as possible in order to reduce noise resulting from layouts in our results. We opted for MDS-based approaches, as they are readily available in all three geometries. Specifically, we use a Euclidean MDS layout from Zheng et al. [ZPG19], spherical MDS from Miller et al. [MHK23], and hyperbolic MDS from Miller et al. [MKH22]. Each of the 9 networks $\times$ 3 geometries $=$ 27 network-layout pairs were visually inspected to ensure they produced reasonable results. A representative example is shown in Fig. 1, and all layouts can be found in supplementary material.

Note that we do not adjust the initial center of networks to account for different questions or different highlighted nodes. This means that some highlighted nodes may be harder to see in spherical and hyperbolic visualizations, but this is an inherent consequence of these visualizations styles and we argue that it makes for a more fair comparison.

Style Edges are 1.5 pixels in width and are grey in color. When an incident node has been hovered over by the participant, the edge doubles in thickness and its color changes to black. We aim to keep node sizes as consistent as possible across each condition, despite the differing behaviour of the geometries. At the exact geometric center of each condition, the node size is precisely 10 pixels. In Euclidean geometry, the size and shape is fixed. Hyperbolic geometry has a strong focus+context with node sizes decreasing as they approach the boundary. In spherical geometry, the circles representing nodes are stretched to ellipses, eventually disappearing "behind" the globe. For some tasks, we ask questions related to "highlighted" nodes, which appear 50% larger in radius than they would otherwise. Each condition has a default white background, with a 1 pixel black border to indicate the visualization space. This border is a rectangle in **E**, but a circle in both **H** and **S** conditions due to the chosen projections. We use colorblind-safe options for the nodes [Won11]: light blue for visualizing nodes by default, yellow for hovered nodes, magenta for neighbors of hovered nodes, and orange for "highlighted" nodes related to the question; see Fig. 2(c). The exact color scheme can be found in supplemental material.

Display As the interactions and feel of the tools were developed with desktop PCs in mind, we decided to restrict the availability of the test on mobile, tablet and other smaller devices. We set the minimum width of a device to be 801 pixels and any device under that measurement would not be able to access any page of the tool. For larger devices, the visualization would fill the dimensions of the window. Controlling the use of such small devices removes a potentially confounding variable in the study.

We note that while the **S** and **H** conditions are contained in a circle, the **E** condition is rectangular. While one could restrict **E** to a circle as well, we decided to keep it as rectangular to preserve external validity of our study. Just as rectangular windows are standard for Euclidean visualizations, circular windows are standard for the orthographic projection of spherical space and the Poincarè projection of hyperbolic space.

3.4. Tasks

In an effort to cover as broad a spectrum of tasks as possible, we use a table that represents the intersection between the network task taxonomy of Lee et al. [LPP*06] and the more general visualization taxonomy of Amar et al. [AES05]; see Table 2. First, we identified where Du et al.'s [DCL*17] three tasks fell in this table, shown in orange (**D1, D2, D3**). We then attempted to cover all columns (all types of network tasks) while covering as many rows as possible. Our experiment utilizes 6 tasks, shown in blue in the table:

- **T1**: Count neighbors of a node with a given degree
- **T2**: Count common neighbors of two nodes
- **T3**: Determine the length of the shortest path between two nodes
- **T4**: Estimate the size (nodes or edges) of the graph
- **T5**: Determine the most frequent degree of a group of nodes
- **T6**: Count how many additional nodes are reachable from a given node in given number of steps

An instance for one of the above tasks is a layout of a network, with highlighted relevant nodes (or node), and 4 possible answers (one of which is correct). The task instances in our study are generated programatically and ensure that there is exactly one correct an-

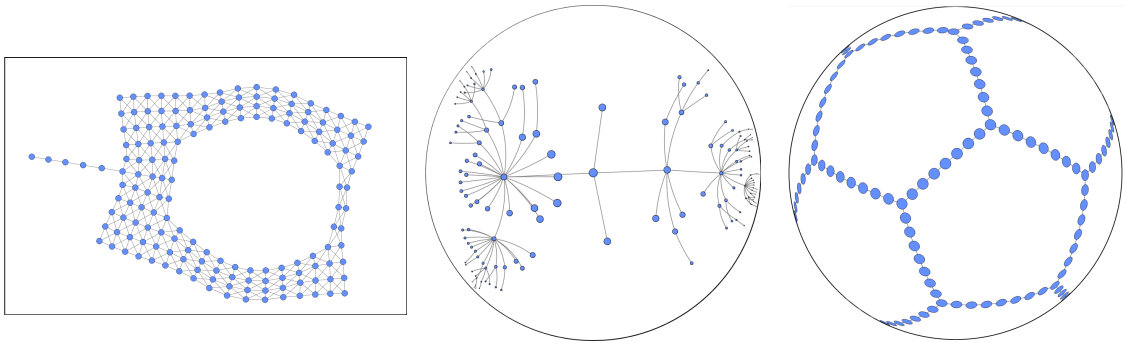

(a) (b) (c)

Figure 4: *(a) dwt_162 shown in the **E** condition (b) tree_150 shown in the **H** condition (c) dodecahedron_3 shown in the **S** condition. Each of these networks are representative of the types of networks which have lowest distortion in their respective spaces.*

swer. We also control the level of difficulty targeting under 30 seconds for completion. Possible answers are always shown in sorted order.

For each network, we create 3 instances for each of our 6 tasks, resulting in $9 \times 6 \times 3 = 162$ total unique instances. An example of one instance of each task is shown in supplemental material and all 162 instances can be found via the web page; see Section 6.

3.5. Experimental design

We created a within-subjects experiment, as it is important to directly compare participant results by geometry. However, the number of network/task/geometry triples ($9 \times 6 \times 3 = 162$) makes the experiment too long for one person. With this in mind, we settled on a within-subjects design with respect to networks and geometry (every participant sees all all networks and all geometries), but broke the tasks into 3 groups of 2 (each participant sees only two of the six tasks). A full within-subjects design took participants too long to complete, so we settled on this shorter study as a compromise.

This results in a design where each participant answers 54 questions (9 networks x 2 tasks x 3 geometries). The order in which participants used each geometry, as well as the order of the questions, is determined based on a balanced Latin square to reduce learning effects i.e. participants were assigned a square for order of geometry, and another square for order of questions.

Experiment outline The experiment design was reviewed and approved by the University of Arizona Institutional Review Board (STUDY00003850). After consenting to participation, the main body of the experiment contains 3 blocks, one per condition.

Each block begins with an introduction page. This page introduces definitions, descriptions of interactions, and an example visualization in the current condition. Participants were encouraged to spend time familiarizing themselves with their specific visualization and interactions using a small sample graph; an example is shown in supplementary material.

After the introduction, each block goes through 18 questions with the current condition, one for each network-task pair. The final question page design is found in supplemental material. After the last task, participants are asked to answer ten subjective questions about the condition (e.g., how aesthetically pleasing was this condition?) on a 1-5 Likert scale. The order of the 3 blocks, as well as the order of the questions within each block, is determined based on a balanced Latin square. The final page of the experiment collects general demographic data (e.g., age group, gender) and provides a window for open-ended feedback.

Amar et al. [AES05]	Lee et al. [LPP*06]					
	Adjacency	Accessibility	Comm. Connect.	Connectivity	Overview
Retrieve Value		T6	T2		
Filter	T1				
Compute Value	T5				
Find Extremum	D1, D3		D2	T3	
Det. Range					T4

Table 2: *Task classification for our tasks and Du et al.'s tasks. Tasks which do not have a row or column filled are omitted.*

Results from Pilot During the design phase, we asked visualization researchers (not involved in the study beyond the pilot) to complete the experiment and provide feedback. This helped catch bugs and minor fixes, but more importantly we were able to identify and rectify several non-trivial issues. We briefly discuss three examples.

One such issue was the pan effect for S and H conditions. Several pilot participants noted that the pan direction felt "inverted" from Euclidean space. While we as designers imagined rotating the ball or hyperbolic plane, this was not how the effect was being perceived. We changed the pan effect so that the pan is always in the direction of the mouse cursor for all conditions. The second issue concerned difficulties finding highlighted nodes (see Fig.2(c)). Based on this feedback, we increased the size of the nodes of interest to allow them to further stand out (in addition to being of different color). Finally, some task instances were too difficult and others too easy. This feedback helped us control the difficulty level across conditions to hopefully avoid floor and ceiling effects.

4. Results and analysis

We recruited participants for the study by making a webpage available on Reddit, posting to subreddits r/takemysurvey and

r/samplesize. We additionally contacted friends and colleagues. No incentives were offered for participation.

Demographics: In total, we had 29 participants complete the study. The average amount of time spent on trials was 25.5 minutes, while the average real-world time (breaks, directions, feedback, etc. included) was 46.2 minutes. Of our participants, 23 were men, 4 were woman, and the remaining 2 preferred not to say. 25 participants were between the ages of 18-35 and the remaining 4 in the ages of 36-55. Familiarity with network visualizations ranged from 4 that were either completely new or had seen networks in passing, to 13 that had discussed networks in coursework, to 6 that use them in their work/job, and 6 participants identified as experts.

4.1. Quantitative analysis

The majority of data collected is not normally distributed, and so non-parametric tests are performed. Unless otherwise specified, the significance level of all tests is done at $p < 0.05$.

Effectiveness is measured in three ways: accuracy, response time, and interactions [HEH09, BHW*21]. Accuracy is a binary measure: 0 if a participant answered incorrectly and 1 if a participant answered correctly. Response time is the amount of time in seconds from when the visualization loads until the participant submits their answer; this includes reading the question, navigating the visualization, counting, etc. Interactions are measured by adding together each of the pan, zoom, and double-click interactions. We considered including the hover interaction in the measure but decided against it as hovering was used almost equally in all three conditions; see Fig. 9 (b).

When aggregating non-normal data, it is often advisable to use the median (as we do for response time data) since it is less sensitive to outliers or skew. However, as accuracy and interactions are discrete, we use the mean when aggregating these measures.

When speaking of confidence intervals (CI), we mean the range of values where the true mean of the population lies with 95% probability. This statistic is computed based on the number of samples and the variance of those samples [Dek05].

4.1.1. RQ1

To explore **RQ1** we first grouped participant responses by visualization condition (**E**, **H**, **S**) and by distortion values (e, h, s) (see the blocks in Table 1) to partition our 27 network-drawing pairs into 9 groups: e(**E**), e(**H**), e(**S**), h(**E**), h(**H**), h(**S**), s(**E**), s(**H**), s(**S**). Here, the group h(**E**) refers to the group of networks which have lower distortion in hyperbolic space (the middle three networks in Table 1) and are drawn in a Euclidean style (condition **E**). In particular, we are interested in how each group of networks compare when employed in different visualization conditions.

Analysis: We aggregate data by taking the mean (accuracy, interactions) or median (time) over all tasks for each of these groups per participant. For each effectiveness measure, we perform a two-way non-parametric Wilcoxon Rank Sum test between each set of networks in its "natural" geometry against one of the other geometries i.e. we test e(**E**) against e(**H**) and e(**E**) against e(**S**) with results in Table 3(a).

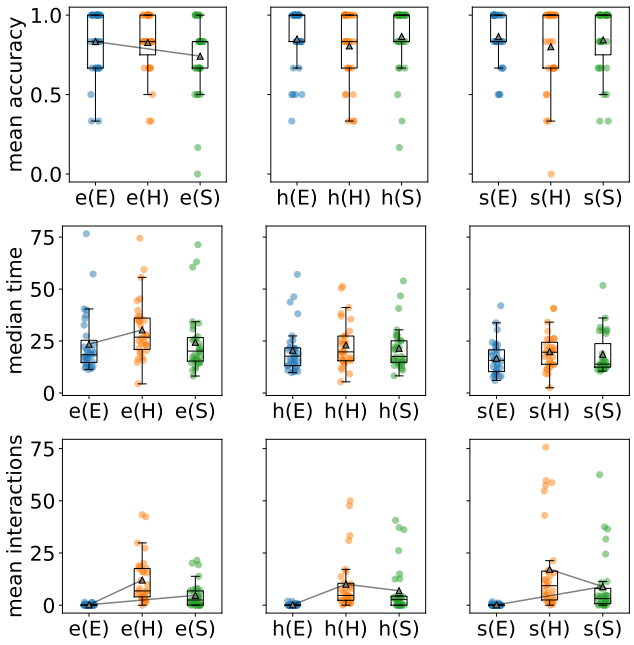

Figure 5: *Relevant statistics for **RQ1** with box plot notation (box shows the first and third quartile of the dataset, inner notch denotes the median, whiskers reach out to furthest datapoint up to 1.5x the length of the box). We have further noted the mean as a grey triangle imposed on the plot. Aggregated individual participant results are shown as semi-transparent points with their x-values randomly perturbed so one can see the distribution. Finally, pairs of groups which are significantly different are shown via a grey line connecting their means. The (top row) show accuracy, (middle row) response time, and (bottom row) interactions.*

For accuracy, one significant difference was found: between e(**E**) and e(**S**). Here, the **S** condition had lower accuracy for these networks. The timing data also indicates a significant result: between e(**E**) and e(**H**), with e(**H**) requiring more time. The interaction data indicates statistically significant differences for every comparison. Boxplots and distributions of the data are found in Fig. 5 and p-values can be found in Table 3(a). Interval plots of the means and CIs are found in supplemental material. Note that since we only make pairwise comparisons, Bonferroni or other statistical corrections are not needed.

Discussion: There is only one significant accuracy result: between e(**E**) and e(**S**). This is possibly due to the sphere "hiding" portions of the network making certain tasks more difficult. Overall, we can conclude that for networks with hyperbolic or spherical structures, the non-Euclidean conditions perform as well as the Euclidean condition in terms of accuracy.

In terms of response time, there is also a single significant result between e(**E**) and e(**H**). For networks with a Euclidean structure, the **E** condition is preferred over **H** as it results in a shorter response time and no accuracy loss. Once again, the lack of other significant results in time shows that the non-Euclidean and Euclidean conditions perform comparably on networks with hyperbolic and spherical structure in terms of time.

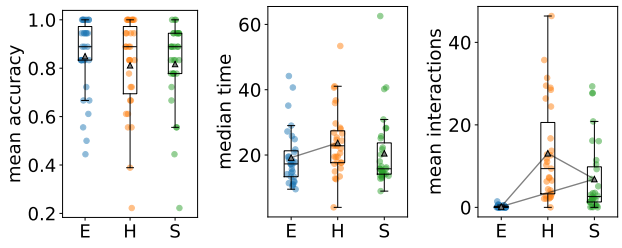

(a) (b) (c)

Figure 6: *Box plots in the same style as Figure 5. Shown here is (a) accuracy, (b) time, and (c) interactions of participant responses over all networks in condition **E**, **H**, and **S**.*

When considering both accuracy and response time, a clear recommendation for visualization designers emerges. For networks with low Euclidean distortion, a Euclidean visualization is ideal as the spherical condition results in lower accuracy and the hyperbolic condition increases response time. However, if a network instead has low hyperbolic or spherical distortion, the **H** and **S** conditions become suitable alternatives as they perform as well as the Euclidean condition. We note however, that while the **H** and **S** conditions are no worse than **E** for these graph types, they are also no better. Thus non-Euclidean visualizations could be viable options, provided good embeddings and interactions.

For interactions (measured by total number of pan, zoom, and double-click events), differences are significant for all tests. However, the order of the means remains consistent (Fig. 5): **E** required the fewest interactions, **S** required more, and **H** required the most. Regardless of distortion values, the interactions required follows this pattern. This suggests that while the non-Euclidean geometries are comparable to Euclidean in terms of performance, they do require more interactions. Note that Euclidean visualizations for smaller networks can be read statically (without any interactions), while the non-Euclidean visualizations require interaction to be effectively read. These results are further confirmed by looking at the average total interactions for each geometry in Fig. 9 (b).

The individual participant data in Fig. 5 offers further insight into significant results. For accuracy, we see that e(**S**) had many answer incorrectly half or more of the time, skewing the distribution downward. Meanwhile for response time, the median of e(**E**) is noticeably earlier than the first quartile of responses in e(**H**).

4.1.2. RQ2

For **RQ2** we are interested in how participants behaved in each visualization condition overall (regardless of network type). Here, instead of the nine groups we created previously we partition into larger groups of three; one for each condition **E**, **H**, **S**.

Analysis: For each condition, we aggregated participant accuracy (mean), response times (median), and interactions (mean), then performed two-way non-parametric Wilcoxon Rank Sum tests to pairwise test (**E** vs.‘**H**), (**E** vs. **S**, and (**H** vs. **S**). We find no significant difference in terms of accuracy. For time, we find a difference between **H** and **S**, with **S** taking less time on average. In terms of interactions, the results are largely the same as before. The p-values are found in Table 3(b) and distributions are shown in Fig. 6.

(a) **RQ1**

	Accuracy	Time	Interactions
e(**E**) vs. e(**H**)	0.972	**0.002**	< **0.001**
e(**E**) vs. e(**S**)	**0.029**	0.608	< **0.001**
h(**H**) vs. h(**E**)	0.273	0.272	< **0.001**
h(**H**) vs. h(**S**)	0.159	0.504	**0.039**
s(**S**) vs. s(**E**)	0.456	0.327	< **0.001**
s(**S**) vs. s(**H**)	0.131	0.555	< **0.001**

(b) **RQ2**

	Accuracy	Time	Interactions
E vs. **H**	0.129	**0.006**	< **0.001**
E vs. **S**	0.065	0.622	< **0.001**
H vs. **S**	0.954	0.094	< **0.001**

Table 3: *Bold values indicate statistical significance. (a) p-values obtained by Wilcoxon tests to address **RQ1**. The distributions can be seen in Fig. 5. The significant results indicate that networks with low Euclidean distortion achieve higher accuracy in the **E** condition compared to **S** and lower response time compared to **H**. However, this advantage of **E** goes away for networks with lower distortion in hyperbolic and spherical spaces. (b) p-value results from Wilcoxon tests for **RQ2** analysis.*

Discussion: Note that when not accounting for network structure, our results of are comparable to those of Du et al. [DCL*17], albeit with smaller networks of different types, and with broader variety of tasks. However, there is one key difference: hyperbolic geometry is not significantly worse in terms of accuracy. We believe this to be due to the improved stress-based layouts and additional interactions. While accuracy is unaffected by the choice of geometry, response times are longer in the **H** condition compared to **E**. When considered alongside our results from **RQ1** the key takeaway is that while hyperbolic visualizations generally perform worse in terms of time than Euclidean ones, there do exist network structures for which Euclidean visualizations do not maintain this advantage. There is no difference from **RQ1** in the analysis for interactions.

4.1.3. RQ3

Here we break up participant responses by visualization condition and by task, creating 3 conditions $\times$ 6 tasks $=$ 18 groups. There are a few results we might expect from prior knowledge. The focus+context of the **H** condition should support adjacency tasks such as **T1** and **T5**. The response times should generally follow the order of **E, H, S**, from shortest to longest. For the overview task, **S** will likely be worse than the rest, as half of the drawing area is hidden.

Analysis: We aggregate participant responses and perform a 3-way non-parametric Friedman test to detect differences between geometries in accuracy and time. We did not detect differences in accuracy, which agrees with our overall results from before. For time, we found two significant result in **T5**. We then conducted a pairwise non-parametric Wilcoxon test at significance level $p < 0.017$ which showed a difference in medians between **E** and **H** as well as **H** and **S**. Notably, **S** took around half as long on average as **H** for **T5** with no loss in accuracy. A similar process found a difference between **H** and **S** for **T2**. See Fig. 7 for response time boxplots; plots for accuracy, as well as interval plots for both accuracy and time, can be found in supplemental material.

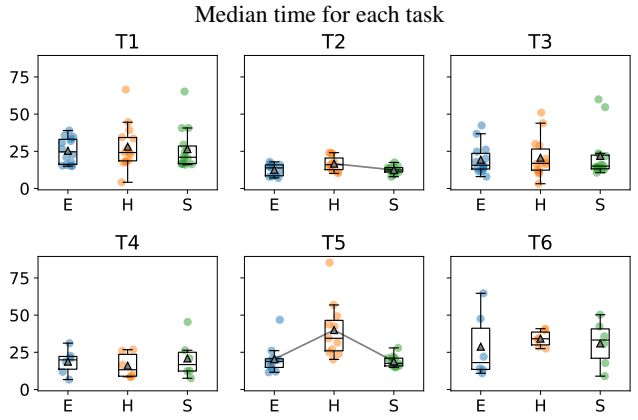

Figure 7: *Box plots in the style of Fig. 5 partitioned by task.*

Discussion: Upon closer examination of the data, we observe some intriguing results that, while not statistically significant, merit attention. Based on prior studies, we expect the accuracy and time to follow the order of **E**, **S** and **H**. However, in certain cases (**T1**, **T3**, **T5**), there is considerable variability in response times for **H**, suggesting that additional training might be necessary to enhance its effectiveness. In **T4**, the overview task, the mean accuracy for **H** and **S** is much worse. This may indicate that the focus+context of non-Euclidean geometries is a poor fit for overview tasks.

We were surprised at the variability of response time between tasks. For instance, in **T5** we have significant results that show **H** required longer response time than either **E** or **S**. It is notable that **S** often had even shorter response time than **E** for this task, though not statistically signicant. A similar pattern can be seen for **T2**. However, it is important to note that our study primarily focuses on **RQ1**, resulting in limited results for individual task performance.

4.2. Subjective Quantitative Feedback

We collected participant feedback using a Likert-scale at the end of each of the 3 blocks (corresponding to the three conditions). We asked for two types of feedback: interaction-related questions and aesthetics-related questions. The first type can help us understand the perceived utility of the provided interactions in the given condition; we can also see if this is correlated to actual use of the interactions. The second type of questions can help see whether personal preferences match the accuracy/time/interaction data. All questions were presented in the same way with the 5 options "Strongly Disagree", "Disagree", "Neutral", "Agree", "Strongly Agree".

4.2.1. Interaction-Related Questions

We collected feedback from participants to express how useful a given interaction was for each condition. The questions were "The *x* interaction assisted answering questions", with the *x* replaced with each of our five measured interactions. We summarize the results of this feedback in Fig. 8; we can clearly see a trend in the usefulness of each interaction. The most useful was the hover interaction, followed by click-and-drag (pan), then by scroll (zoom), then by double-click (recenter) and finally reset. Looking at each geometry, we can see that participants reported interactions were more

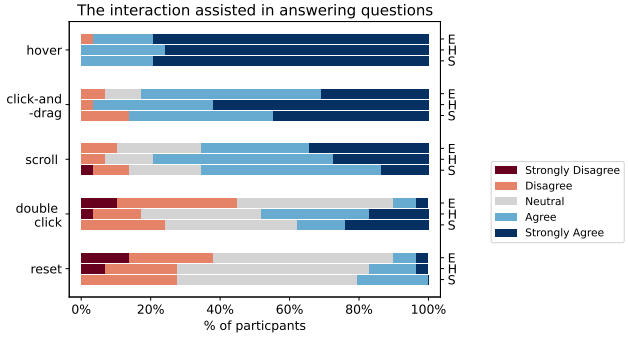

Figure 8: *Responses from all participants regarding interaction-related feedback Exact wording of questions is shown along the y-axis, while the width of a bar on the x-axis is proportional to the percentage of responses on the Likert scale. Each triple of bars is ordered from top to bottom as questions about the **E**, **H**, and **S** conditions respectively. Bands with large amounts of blue indicate mostly positive responses, while red indicates negative responses.*

useful in the **H** condition. Conversely, the **E** condition was helped less through interactions.

To verify these visual results, we conduct a statistical analysis of the responses to detect any significant difference. We conduct a 3-way Friedman test, followed by pairwise 2-way Wilcoxon tests at significance level $p < 0.01$. Of these, only the double-click question had significant difference in mean with **E** against **H** being different at $p = 0.003$ as well as **E** against **S** being different at $p = 0.005$. This result is in agreement with our interaction counts and qualitative feedback; the double-click feature was rarely used in **E**. The remaining results were not significant; see supplemental material.

4.2.2. Aesthetics-Related Questions

We collected feedback on a five point Likert scale from participants on their subjective thoughts and preferences for each condition. The prompts are found and results summarized in Fig. 9(a). Overall, participants had neutral to good reactions to each geometry, with some negative responses for non-Euclidean geometries.

We again conduct a statistical analysis in the same form as before. Only one test resulted in significance: between **E** and **H** ($p = 0.003$) in the question "The visualization style was easy to read and understand." In contrast to the subjective feedback from Du et al. [DCL*17] where **S** was consistently close to **E** in preference and in task support, our results indicate that **S**, **H** and **E** are comparable and **H** does not conspicuously lag behind the other two.

4.3. Qualitative Feedback

We asked participants for additional feedback. The exact prompts and detailed responses are found in supplemental material. Many participants commented on the provided interactions, notably finding the **Hover** and **Pan** interaction helpful, one reporting,

> *I rely heavily on the hovering tool ... I also use the double-click feature (to) often center the target node ....*

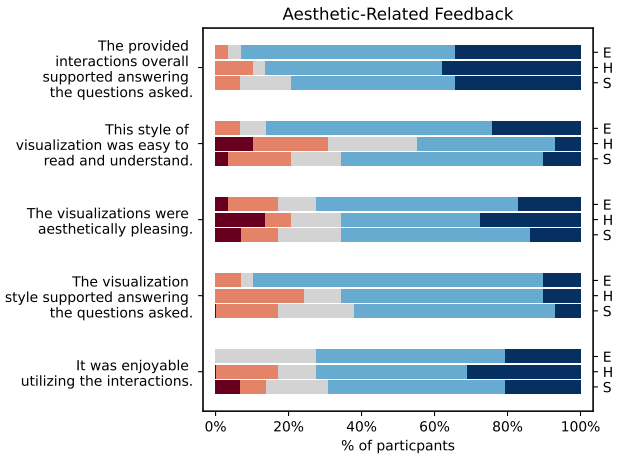

Figure 9: *The aesthetic related feedback in the style of Fig. 8.*

A few participants also mentioned the zoom and recenter interactions in their responses. The type of tasks participants were asked to complete influenced their strategy. An instance of a comment left by a participant placed in the task group with **T3** and **T5** is,

> *Find the point, then use the hover to determine neighbors. For the shortest path found the most direct path. For the neighbors, just hovered to find the neighbors then went through each neighbor, hovered and counted the degree.*

The feedback left by participants reconfirms our results regarding the use of interactions with different visualizations.

5. Limitations

Our results indicate that, with appropriate interactions, non-Euclidean network representations can be competitive in terms of time and accuracy to Euclidean representations. This observation is limited by the nature of the experiment, which relies on a handful of networks with particular structure. Specifically, we generated network embeddings whose distortion matched a particular geometry (e.g., spherical networks with lower distortion in spherical space). Due to this design decision, we cannot say whether or not our results are applicable to real-world graphs, although many real-world graphs exhibit spherical (e.g. geographic) or hyperbolic [KPK*10] geometry. However, even for these networks, the corresponding geometry was only competitive and did not show a clear advantage. Therefore, we simply recommend considering these non-Euclidean visualization styles as viable alternatives to traditional ones in interactive settings.

A few participants highlighted problems they encountered. For instance, one reported that the zoom and pan interactions "felt weird" or were "unintuitive" for the **H** and **S** conditions. Another reported that there were instances of node-edge and edge-edge overlap which increased difficulty. Such issues could have been addressed with more training (allowing participants to get more comfortable with the non-standard conditions). More details can be found in supplemental material.

We only required that a network embedding was lowest in the specified geometry, but did not control for the magnitude of difference. For the network E_rand_small, the Euclidean distortion was 0.10 while the hyperbolic distortion was 0.13. Without knowing how the distortion metric is distributed, it is hard to say whether or not these differences in distortion are significant. We leave a thorough characterization of the distortion metric, such as those for edge crossings, neighborhood preservation etc. in Mooney et al. [MPWK24]), as future work.

As our experiment is within-subjects/between-tasks, each participant worked with only 2/6 tasks. Further, the total number of participants per task was low (9 or 10). More participants would have strengthened our conclusions. Because our tasks cover the spectrum of network tasks, grouping them into pairs might have had an impact. Specifically, as an overview task **T4** is quite different from the rest. There are no highlighted nodes and overview tasks are not as commonly done on the smaller network sizes that appeared in our study. This may have had an effect on participants that saw **T4**.

The relatively large variance for time (see Fig. 6) in the **H** condition might indicate that participants did not receive enough training to be comfortable working in that condition. While it is believable that hyperbolic representations take longer on average, with proper training this might be remedied. Our training was unstructured and identical for each condition; we therefore have no information as to how much (or how quickly) the participants learned how to use the different conditions. Finally, our participants are a biased sample with the majority being young men with some network/graph experience. A more diverse set of participants would help with the generalizability of the results.

6. Conclusion

We aimed to extend prior non-Euclidean network visualization human subjects studies such as [DCL*17] to understand the role of such tools in the broader network visualization field. The trials of our experiment can be found online `https://jacoblmiller.github.io/riemann-study-web/`.

Several open questions remain. First, **RQ3** was not fully answered in this work, and further studies are needed to determine which tasks are best suited to different geometries. Additionally, we did not explore toroidal layouts. Finally, we would like to investigate what other types of data are well-suited for visualization using non-Euclidean geometries.

The key takeaway is that designers can be more confident in choosing a non-Euclidean representation when they want to. For instance, if the data is geographical, maybe one would want to use an interactive "globe-like" representation instead of the usual 2D projection. If the data has interesting local structures but is large or has a hierarchical structure, then one might want to use a hyperbolic representation for its focus+context effect.

To summarize our results, non-Euclidean network representations, obtained by native-to-the-geometry embeddings, and with sufficient interaction support, can be viable alternatives to Euclidean representations.

Acknowledgements

Open Access funding enabled and organized by Projekt DEAL.

References

[AES05] AMAR R. A., EAGAN J., STASKO J. T.: Low-level components of analytic activity in information visualization. In *IEEE Symposium on Information Visualization (InfoVis 2005), 23-25 October 2005* (Minneapolis, MN, USA, 2005), Stasko J. T., Ward M. O., (Eds.), IEEE Computer Society, pp. 111–117. doi:10.1109/INFVIS.2005.1532136. 3, 5, 6

[BHW*21] BURCH M., HUANG W., WAKEFIELD M., PURCHASE H. C., WEISKOPF D., HUA J.: The state of the art in empirical user evaluation of graph visualizations. *IEEE Access 9* (2021), 4173–4198. doi:10.1109/ACCESS.2020.3047616. 7

[CDBM21] CHEN K., DWYER T., BACH B., MARRIOTT K.: It's a wrap: Toroidal wrapping of network visualisations supports cluster understanding tasks. In *CHI '21: CHI Conference on Human Factors in Computing Systems* (2021), ACM. doi:10.1145/3411764.3445439. 1, 3

[CDMB20] CHEN K., DWYER T., MARRIOTT K., BACH B.: Doughnets: Visualising networks using torus wrapping. In *CHI '20: CHI Conference on Human Factors in Computing Systems* (2020), ACM. 1

[CDY*22] CHEN K., DWYER T., YANG Y., BACH B., MARRIOTT K.: Gan'sda wrap: Geographic and network structured data on surfaces that wrap around. In *CHI '22: CHI Conference on Human Factors in Computing Systems, New Orleans, LA, USA, 29 April 2022 - 5 May 2022* (2022), Barbosa S. D. J., Lampe C., Appert C., Shamma D. A., Drucker S. M., Williamson J. R., Yatani K., (Eds.), ACM, pp. 135:1–135:16. doi:10.1145/3491102.3501928. 1, 2, 3

[CHE22] CHEN K.-T.: *It's a Wrap! Visualisations that Wrap Around Cylindrical, Toroidal, or Spherical Topologies*. PhD thesis, Monash University, 8 2022. doi:10.26180/20723092.v1. 3

[DCL*17] DU F., CAO N., LIN Y., XU P., TONG H.: iSphere: Focus+context sphere visualization for interactive large graph exploration. In *Proceedings of the 2017 CHI Conference on Human Factors in Computing Systems, Denver, CO, USA, May 06-11, 2017* (2017), Mark G., Fussell S. R., Lampe C., m. c. schraefel, Hourcade J. P., Appert C., Wigdor D., (Eds.), ACM, pp. 2916–2927. doi:10.1145/3025453.3025628. 1, 2, 3, 4, 5, 8, 9, 10

[Dek05] DEKKING F. M.: *A Modern Introduction to Probability and Statistics: Understanding why and how*. Springer Science & Business Media, 2005. 7

[EMK*21] ESPADOTO M., MARTINS R. M., KERREN A., HIRATA N. S. T., TELEA A. C.: Toward a quantitative survey of dimension reduction techniques. *IEEE Trans. Vis. Comput. Graph. 27*, 3 (2021), 2153–2173. doi:10.1109/TVCG.2019.2944182. 1, 2

[GKN04] GANSNER E. R., KOREN Y., NORTH S.: Graph drawing by stress majorization. In *International Symposium on Graph Drawing* (2004), Springer, pp. 239–250. 2, 3

[GSF97] GROSS M. H., SPRENGER T. C., FINGER J.: Visualizing information on a sphere. In *Proceedings of VIZ'97: Visualization Conference, Information Visualization Symposium and Parallel Rendering Symposium* (1997), IEEE, pp. 11–16. doi:10.1109/INFVIS.1997.636759. 1, 2

[HEH09] HUANG W., EADES P., HONG S.: Measuring effectiveness of graph visualizations: A cognitive load perspective. *Inf. Vis. 8*, 3 (2009), 139–152. doi:10.1057/IVS.2009.10. 7

[JLK*25] JEON H., LEE H., KUO Y.-H., YANG T., ARCHAMBAULT D., KO S., FUJIWARA T., MA K.-L., SEO J.: Unveiling high-dimensional backstage: A survey for reliable visual analytics with dimensionality reduction. In *CHI '25: CHI Conference on Human Factors in Computing Systems* (2025), ACM. doi:10.48550/arXiv.2501.10168. 3

[KK89] KAMADA T., KAWAI S.: An algorithm for drawing general undirected graphs. *Inf. Process. Lett. 31*, 1 (1989), 7–15. doi:10.1016/0020-0190(89)90102-6. 2

[KPK*10] KRIOUKOV D., PAPADOPOULOS F., KITSAK M., VAHDAT A., BOGUNÁ M.: Hyperbolic geometry of complex networks. *Physical Review E 82*, 3 (2010), 036106. 4, 5, 10

[Kru64] KRUSKAL J. B.: Multidimensional scaling by optimizing goodness of fit to a nonmetric hypothesis. *Psychometrika 29*, 1 (1964), 1–27. 1

[KW05] KOBOUROV S., WAMPLER K.: Non-Euclidean spring embedders. *IEEE Trans. Vis. Comput. Graph. 11*, 6 (2005), 757–767. doi:10.1109/TVCG.2005.103. 1, 2, 3

[LPP*06] LEE B., PLAISANT C., PARR C. S., FEKETE J.-D., HENRY N.: Task taxonomy for graph visualization. In *Proceedings of the 2006 AVI Workshop on BEyond Time and Errors: Novel Evaluation Methods for Information Visualization* (New York, NY, USA, 2006), BELIV '06, Association for Computing Machinery, p. 1–5. doi:10.1145/1168149.1168168. 3, 5, 6

[LRP95] LAMPING J., RAO R., PIROLLI P.: A focus+context technique based on hyperbolic geometry for visualizing large hierarchies. In *Human Factors in Computing Systems, CHI '95 Conference Proceedings* (1995), ACM/Addison-Wesley, pp. 401–408. doi:10.1145/223904.223956. 1, 2

[MB95] MUNZNER T., BURCHARD P.: Visualizing the structure of the world wide web in 3d hyperbolic space. In *Procedings of the 1995 Symposium on Virtual Reality Modeling Language* (1995), ACM, pp. 33–38. doi:10.1145/217306.217311. 1, 2

[MBK24] MILLER J., BHATIA D., KOBOUROV S.: State of the art of graph visualization in non-Euclidean spaces. In *Computer Graphics Forum* (2024), vol. 43, Wiley Online Library, p. e15113. doi:10.1111/cgf.15113. 2

[MCH*09] MOSCOVICH T., CHEVALIER F., HENRY N., PIETRIGA E., FEKETE J.: Topology-aware navigation in large networks. In *Proceedings of the 27th International Conference on Human Factors in Computing Systems, CHI 2009, Boston, MA, USA, April 4-9, 2009* (2009), Jr. D. R. O., Arthur R. B., Hinckley K., Morris M. R., Hudson S. E., Greenberg S., (Eds.), ACM, pp. 2319–2328. doi:10.1145/1518701.1519056. 4

[MHK23] MILLER J., HUROYAN V., KOBOUROV S.: Spherical graph drawing by multi-dimensional scaling. In *Graph Drawing and Network Visualization: 30th International Symposium, GD 2022, Tokyo, Japan, September 13–16, 2022, Revised Selected Papers* (2023), Springer, pp. 77–92. doi:10.1007/978-3-031-22203-0_7. 2, 3, 4, 5

[MKH22] MILLER J., KOBOUROV S. G., HUROYAN V.: Browser-based hyperbolic visualization of graphs. In *15th IEEE Pacific Visualization Symposium, PacificVis 2022, Tsukuba, Japan, April 11-14, 2022* (2022), IEEE, pp. 71–80. doi:10.1109/PACIFICVIS53943.2022.00016. 1, 2, 3, 4, 5

[MPW*24] MOONEY G. J., PURCHASE H. C., WYBROW M., KOBOUROV S. G., MILLER J.: The perception of stress in graph drawings. In *32nd International Symposium on Graph Drawing and Network Visualization (GD 2024)* (2024), Schloss Dagstuhl–Leibniz-Zentrum für Informatik, pp. 21–1. doi:10.4230/LIPIcs.GD.2024.21. 2

[MPWK24] MOONEY G. J., PURCHASE H. C., WYBROW M., KOBOUROV S. G.: The multi-dimensional landscape of graph drawing metrics. In *2024 IEEE 17th Pacific Visualization Conference (PacificVis)* (2024), IEEE, pp. 122–131. doi:10.1109/PacificVis60374.2024.00022. 10

[Mun97] MUNZNER T.: H3: laying out large directed graphs in 3D hyperbolic space. In *IEEE Symposium on Information Visualization* (1997), IEEE Computer Society, pp. 2–10. doi:10.1109/INFVIS.1997.636718. 1, 2

[PCZ*21] PAN J., CHEN W., ZHAO X., ZHOU S., ZENG W., ZHU M., CHEN J., FU S., WU Y.: Exemplar-based layout fine-tuning for node-link diagrams. *IEEE Trans. Vis. Comput. Graph. 27*, 2 (2021), 1655–1665. doi:10.1109/TVCG.2020.3030393. 4

[Pen03] PENROSE M.: *Random Geometric Graphs*. Oxford University Press, 05 2003. doi:10.1093/acprof:oso/9780198506263.001.0001. 4

[PYGK20] PERRY S., YIN M. S., GRAY K., KOBOUROV S.: Drawing graphs on the sphere. In *AVI '20: International Conference on Advanced Visual Interfaces* (2020), ACM, pp. 17:1–17:9. 2

[SB94] SARKAR M., BROWN M. H.: Graphical fisheye views. *Commun. ACM 37*, 12 (1994), 73–84. doi:10.1145/198366.198384. 3

[SK03] SANGOLE A. P., KNOPF G. K.: Visualization of randomly ordered numeric data sets using spherical self-organizing feature maps. *Comput. Graph. 27*, 6 (2003), 963–976. doi:10.1016/J.CAG.2003.08.012. 1, 2

[SSGR18] SALA F., SA C. D., GU A., RÉ C.: Representation tradeoffs for hyperbolic embeddings. In *Proceedings of the 35th International Conference on Machine Learning* (2018), vol. 80 of *Proceedings of Machine Learning Research*, PMLR, pp. 4457–4466. 1, 2

[SZG*96] SCHAFFER D., ZUO Z., GREENBERG S., BARTRAM L., DILL J., DUBS S., ROSEMAN M.: Navigating hierarchically clustered networks through fisheye and full-zoom methods. *ACM Trans. Comput. Hum. Interact. 3*, 2 (1996), 162–188. doi:10.1145/230562.230577. 4

[Tor52] TORGERSON W. S.: Multidimensional scaling: I. theory and method. *Psychometrika 17*, 4 (1952), 401–419. 2

[WB05] WARE C., BOBROW R. J.: Supporting visual queries on medium-sized node-link diagrams. *Inf. Vis. 4*, 1 (2005), 49–58. doi:10.1057/PALGRAVE.IVS.9500090. 4

[Won11] WONG B.: Points of view: Color blindness. *Nature methods 8* (06 2011), 441. doi:10.1038/nmeth.1618. 5

[WT06] WU Y., TAKATSUKA M.: Visualizing multivariate network on the surface of a sphere. In *Proceedings of the 2006 Asia-Pacific Symposium on Information Visualisation-Volume 60* (2006), pp. 77–83. URL: https://dl.acm.org/citation.cfm?id=1151915. 2

[WWZ*19] WANG Y., WANG Y., ZHANG H., SUN Y., FU C., SEDLMAIR M., CHEN B., DEUSSEN O.: Structure-aware fisheye views for efficient large graph exploration. *IEEE Trans. Vis. Comput. Graph. 25*, 1 (2019), 566–575. doi:10.1109/TVCG.2018.2864911. 3, 4

[YAD*18] YOGHOURDJIAN V., ARCHAMBAULT D., DIEHL S., DWYER T., KLEIN K., PURCHASE H. C., WU H.: Exploring the limits of complexity: A survey of empirical studies on graph visualisation. *Vis. Informatics 2*, 4 (2018), 264–282. doi:10.1016/J.VISINF.2018.12.006. 2

[ZPG19] ZHENG J. X., PAWAR S., GOODMAN D. F. M.: Graph drawing by stochastic gradient descent. *IEEE Trans. Vis. Comput. Graph. 25*, 9 (2019), 2738–2748. doi:10.1109/TVCG.2018.2859997. 2, 5